Aneustat (OMN54) has aerobic glycolysis-inhibitory activity and also immunomodulatory activity as indicated by a first-generation PDX prostate cancer model

Sifeng Qu[1,2,3,4], Hui Xue[1], Xin Dong[1], Dong Lin[1,2], Rebecca Wu[1], Noushin Nabavi[2], Colin C. Collins[2,4], Martin E. Gleave[2,4], Peter W. Gout[1] and Yuzhuo Wang [1,2,3,4]

[1] Department of Experimental Therapeutics, BC Cancer Agency, Vancouver, BC, Canada

[2] Vancouver Prostate Centre, Vancouver, BC, Canada

[3] Interdisciplinary Oncology Program, Faculty of Medicine, University of British Columbia, Vancouver, BC, Canada

[4] Department of Urologic Sciences, Faculty of Medicine, University of British Columbia, Vancouver, BC, Canada

Aneustat (OMN54) is a multivalent, botanical anticancer candidate therapeutic. A recent Phase-I clinical trial has indicated that it is well tolerated by patients and has immunomodulatory activity. In our study, using *in vitro* and *in vivo* prostate cancer models, we investigated Aneustat with regard to effects on (i) cancer-generated immunosuppression based on aerobic glycolysis leading to acidification of the tumor microenvironment, and (ii) immune-related processes such as macrophage differentiation and shifts in the intratumoral levels of host immune cells. Aneustat markedly reduced glucose consumption, lactic acid secretion, glycolysis-related gene expressions and proliferation of human LNCaP prostate cancer cells. In addition, Aneustat induced differentiation of RAW264.7 macrophages to the M1 anticancer phenotype. Treatment of LNCaP xenografts and first-generation patient-derived prostate cancer tissue xenografts with Aneustat in both cases led to a marked shift in intratumoral host (mouse/patient) immune cell levels: a higher ratio of cytotoxic CD8$^+$ T/Treg cells, higher numbers of NK cells, lower numbers of Treg cells and MDSCs, i.e. changes favoring the host anticancer immune response. Taken together, the data indicate that Aneustat has immunomodulatory activity based on inhibition of aerobic glycolysis which in patients may lead to reduction of cancer-induced immunosuppression. Furthermore, first-generation patient-derived cancer tissue xenograft models may be used for screening compounds for immunomodulatory activity.

Introduction

It is well recognized that the immune system has a dual role in cancer development, as cancers characteristically contain a variety of host immune cells that can either inhibit or promote cancer growth.[1,2] On one hand, intratumoral CD8$^+$ T cells, NK cells and M1 macrophages, i.e. major effector cells of the host anticancer immune response, are aimed at eliminating cancer cells.[2,3] On the other hand, tumors also contain immunosuppressive cells, such as regulatory T cells (Tregs), myeloid-derived suppressive cells (MDSCs) and M2 macrophages, that can promote cancer development by suppressing the host anticancer immune response.[3] Unfortunately, as cancers progress, intratumoral cancer-induced immunosuppression becomes dominant.[4] Recent successes in cancer immunotherapy based on stimulation of the host anticancer immune response have underlined the importance of the latter in the fight against the disease.[5]

There is compelling evidence that epithelial cancers can suppress the anticancer immune response of the host by various mechanisms.[6] Thus reprogramed glucose metabolism, i.e. aerobic glycolysis, which is commonly used by cancer cells, leads to increased lactic acid secretion and a subsequent low, immune function-inhibiting pH in their environment.[7,8] The acidification of the tumor microenvironment can suppress the host anticancer immune response as it has been found to promote

What's new?

Aneustat is a first-in-class multivalent, botanical immuno-oncology candidate therapeutic; as indicated by a recent Phase-I trial, it is well-tolerated by patients. But the mechanisms of action underlying its immunomodulatory activity remain unclear. Using a first-generation patient-derived prostate cancer tissue xenograft model, the authors found that treatment with Aneustat induced a shift in the levels of intra-tumoral patient immune cells, favoring the host anticancer immune response considered critical for cancer treatment. This immunomodulatory activity appears to be based on inhibition of aerobic glycolysis resulting in reduced acidification of the tumor microenvironment, which in patients may lead to reduction of cancer-induced immunosuppression.

expansion of intratumoral numbers of Treg cells and MDSCs and reduce intratumoral levels of CD8^{+} T cells and NK cells,[9,10] resulting in a lower ratio of intratumoral CD8^{+} T cells to Treg cells as observed in cancers of patients.[11] Such a role of cancer-generated lactic acid has been demonstrated using B16 mouse melanoma allografts in immunocompetent C57BL/6 and Rag2^{−/−} mice. Thus a reduction of lactic acid secretion by the tumors, obtained by specific depletion of lactate dehydrogenase-A (LDHA), led to lower numbers of intratumoral MDSCs and higher numbers of intratumoral NK cells and CD8^{+} T cells compared to controls.[10] As such, targeting aerobic glycolysis to reduce lactic acid secretion by cancer cells appears to be a useful strategy for restoring the host anticancer immune response.[7,8] This would lead to a higher ratio of CD8^{+} T cells to Treg cells, a higher number of NK cells and a lower number of MDSCs – a signature associated with improved patient outcome.[12–15]

Aneustat (OMN54) is a first-in-class multivalent immuno-oncology therapeutic, i.e. a mixture of extracts of Ganoderma lucidum, Salvia miltiorrhiza and Scutellaria barbata with anticancer activity, developed by Omnitura Therapeutics, Inc., USA. Recently, a Phase-I Clinical Trial (NCTId: NCT01555242) has shown that Aneustat was well tolerated by patients. Furthermore, treatment with Aneustat led to a decrease in the levels of immune suppression markers in patients (e.g., TGF-β),[16] indicative of an Aneustat-induced reduction in cancer-induced immunosuppression. As well, preliminary preclinical studies have indicated that Aneustat has anti-inflammatory and immunomodulatory activities.[17] We have recently demonstrated, using a patient-derived prostate cancer xenograft model, that combining docetaxel (used in first-line treatment of advanced prostate cancer) with Aneustat led to much higher antitumor activity than the combined activities of the individual drugs, with indications that inhibition of aerobic glycolysis was involved.[18]

In our study, we investigated Aneustat with regard to effects on (i) aerobic glycolysis of LNCaP prostate cancer cells, a process underlying cancer-generated lactic acid-induced immunosuppression and (ii) immune system-related processes such as macrophage differentiation and shifts in the levels of intratumoral host immune cells using LNCaP xenografts and first-generation patient-derived prostate cancer tissue xenografts.

Materials and Methods
Materials
Chemicals, solvents and solutions were obtained from Sigma-Aldrich, Oakville, Canada, unless otherwise indicated.

Aneustat was supplied by Omnitura Therapeutics, Inc. (Henderson, NV).

Gene set enrichment analysis (GSEA)
GSEA is a computational method that uses statistical approaches to identify significantly enriched or depleted groups of genes between two biological states/groups.[19,20]

Cell cultures
Human LNCaP prostate cancer cells and mouse RAW264.7 macrophages were purchased from the American Type Culture Collection (ATCC; Manassas, VA). The cell lines were maintained as monolayer cultures in RPMI-1640 medium (GE Healthcare HyClone; Mississauga, Canada) and DMEM medium (GE Healthcare HyClone), respectively, supplemented with fetal bovine serum (FBS 10%; GE Healthcare HyClone), at 37°C in a humidified incubator with a 5% CO_2/air atmosphere. Cells were trypsinized to form a single cell suspension and counted using a TC20 Automated Cell Counter (Bio-Rad; Mississauga, Canada). Cell viability was determined by Trypan blue exclusion.

Treatment of LNCaP and RAW264.7 cell cultures with Aneustat
LNCaP and RAW264.7 single cell suspensions were seeded into six-well culture plates (starting concentration ∼2.5 × 10^5 cells/well for LNCaP cells and ∼2 × 10^5 cells/well for RAW264.7 cells) and incubated at 37°C in 5% CO_2/air for 18 hr. Aneustat (dissolved in DMSO + Ethanol) or vehicle control (DMSO + Ethanol) were then added to the cultures for a further 48 hr incubation to assess the effects of Aneustat.

Quantitative real-time PCR
Total RNA was isolated using the RNeasy Mini Kit (Qiagen, Inc.; Toronto, Canada) and cDNA was synthesized using the QuantiTect Reverse Transcription Kit (Qiagen, Inc.) according to the manufacturer's instructions. Primers used were described in Supporting Information Table S1. qRT-PCR reactions using KAPA SYBR FAST Universal (Kapa Biosystems; Wilmington, MA) were performed in triplicate in a ViiA 7 Real-Time PCR System (Applied Biosystems; Foster City, CA). Expression levels of genes were normalized to HRPT1/Hprt1.

Western blot analysis
LNCaP cells were treated with vehicle control and Aneustat for 48 hr; whole cell protein extracts were resolved on SDS-

PAGE using procedures previously reported.[8] Proteins were then transferred to PVDF membranes. After blocking for 1 hr at room temperature in 5% milk in TBS/0.1% Tween-20, membranes were incubated overnight at 4°C with appropriate primary antibodies. Following incubation with secondary antibody, immunoreactive proteins were visualized with a SuperSignal™ West Femto Maximum Sensitivity Substrate (Thermo Scientific; Rockford, IL). The following antibodies were used: anti-GLUT1 (ab115730, rabbit monoclonal antibody, Abcam; Toronto, Canada); anti-LDHA (3582, rabbit monoclonal antibody, Cell Signaling Technology; Beverly, MA); anti-MCT4 (sc-50329, rabbit polyclonal antibody, Santa Cruz; Mississauga, Canada); anti-actin (A2066, rabbit polyclonal antibody, Sigma). Actin was used to monitor the amounts of samples applied.

Glucose consumption and lactate secretion determinations

LNCaP cells and RAW264.7 cells, treated with Aneustat for 48 hr or vehicle control, were assessed for glucose consumption and lactate secretion after another 8 hr incubation in fresh medium. Samples of the media were then taken and deproteinized with 10 K Spin Columns (BioVision; Milpitas, CA) prior to determination of glucose and lactate concentration using Glucose Assay Kit and Lactate Assay Kit (BioVision) as previously described.[8] Final concentrations of glucose and lactate were determined by normalizing to the total number of live cells.

ELISA of TNF-α secretion

RAW264.7 cells, treated for 48 hr with Aneustat or vehicle control, were used for TNF-α secretion assessment after another 8 hr incubation in fresh medium. Samples of the media were then taken and the TNF-α concentration was determined using Mouse TNF ELISA Set II (558534, BD Biosciences; Mississauga, Canada) following the manufacturer's instructions. The final concentration of secreted TNF-α was normalized to the total number of live cells.

Animals

Athymic nude mice and NOD/SCID-IL-2R-γc-KO (NOG or NSG) mice, bred in the BC Cancer Research Centre ARC animal facility (Vancouver, Canada), were housed in sterile microisolator cages under specific pathogen-free conditions. Food and water were sterilized prior to use. Temperature (20–21°C) and humidity (50–60%) were controlled. Daily light cycles were 12 hr light and 12 hr dark. Cages were completely changed once or twice a week. Animals were handled under sterile conditions. Animal care and experiments were carried out in accordance with the guidelines of the Canadian Council on Animal Care.

LNCaP xenograft mouse model and treatment with Aneustat

LNCaP cells (in 1:1 HBSS:Matrigel) were grafted under renal capsules of male athymic nude mice (Simonsen Laboratories; Gilroy, CA; 2 groups; 5 mice/group; 4 grafts/mouse). Three

weeks after engraftment, the mice were randomly distributed into two groups and treated with Aneustat (1,652 mg/kg; orally; Q1d × 5/3) or vehicle control (Tween 80 in saline solution; orally; Q1d × 5/3). The health of the mice was monitored daily. After 3 weeks, the mice were euthanized and tissue sections prepared for histopathological analysis.

First-generation patient-derived prostate cancer xenograft model, treatment with Aneustat

Fresh patient metastatic prostate cancer lymph node tissues (obtained from the Vancouver General Hospital with proper patients' consent and approved biosafety certificates and animal protocols) were grafted under renal capsules of male NOD/SCID-IL-2R-γc-KO (NOG or NSG) mice supplemented with testosterone as previously described.[18] After 10 days, the mice were randomly divided into two groups (3 mice/group; 4 grafts/mouse), and treated with Aneustat (1,652 mg/kg; orally; Q1d × 5/3) or vehicle control (orally; Q1d × 5/3). The health of the mice was monitored daily. After 3 weeks, the mice were euthanized and tissue sections prepared for histopathological analysis.

Immunohistochemical staining

Paraffin-embedded tissue sections were prepared and immunohistochemical analyses were performed as previously described.[21] Anti-mouse NK1.1 (CL8994AP, Cedarlane; Burlington, Canada), anti-mouse Ly6G (127601, Biolegend; San Diego, CA), anti-human CD8 (ab93278, Abcam; Toronto, Canada), anti-human Foxp3 (14–7979, eBioscience; San Diego, CA), anti-human CD33 (ab199432, Abcam) and anti-human NCR1 (ab14823, Abcam) antibodies were used for immunohistochemical staining. Three fields of each slide showing positively stained intratumoral lymphocytes were selected and images taken (×400 for LNCaP xenografts and ×200 for first-generation patient-derived tumor tissue xenografts),[22,23] using an AxioCam HR CCD mounted on an Axioplan 2 microscope and ZEN 2.3 software (Carl Zeiss; Toronto, Canada). Positively stained cells in each image were counted. Prior to use, antibodies were tested for target and species specificity.

Statistics

Statistical analysis was determined using GraphPad Prism 5 (GraphPad Software, Inc.; La Jolla, CA); otherwise the Student's *t*-test was used. Results were considered statistically significant when $p < 0.05$ and are expressed as means ± SEM.

Results

Gene set enrichment analysis of gene expression profiles of patient-derived prostate cancer tissue xenografts from Aneustat-treated and control groups

Microarray data, obtained in a previous study of LTL-313H patient-derived prostate cancer xenografts treated with Aneustat (GSE48667), were filtered by removal of probes without corresponding gene annotations and probes without detectable expression levels (<4 in log2 scale) as previously described.[18] The gene enrichment was analyzed using GSEA hallmark gene-set
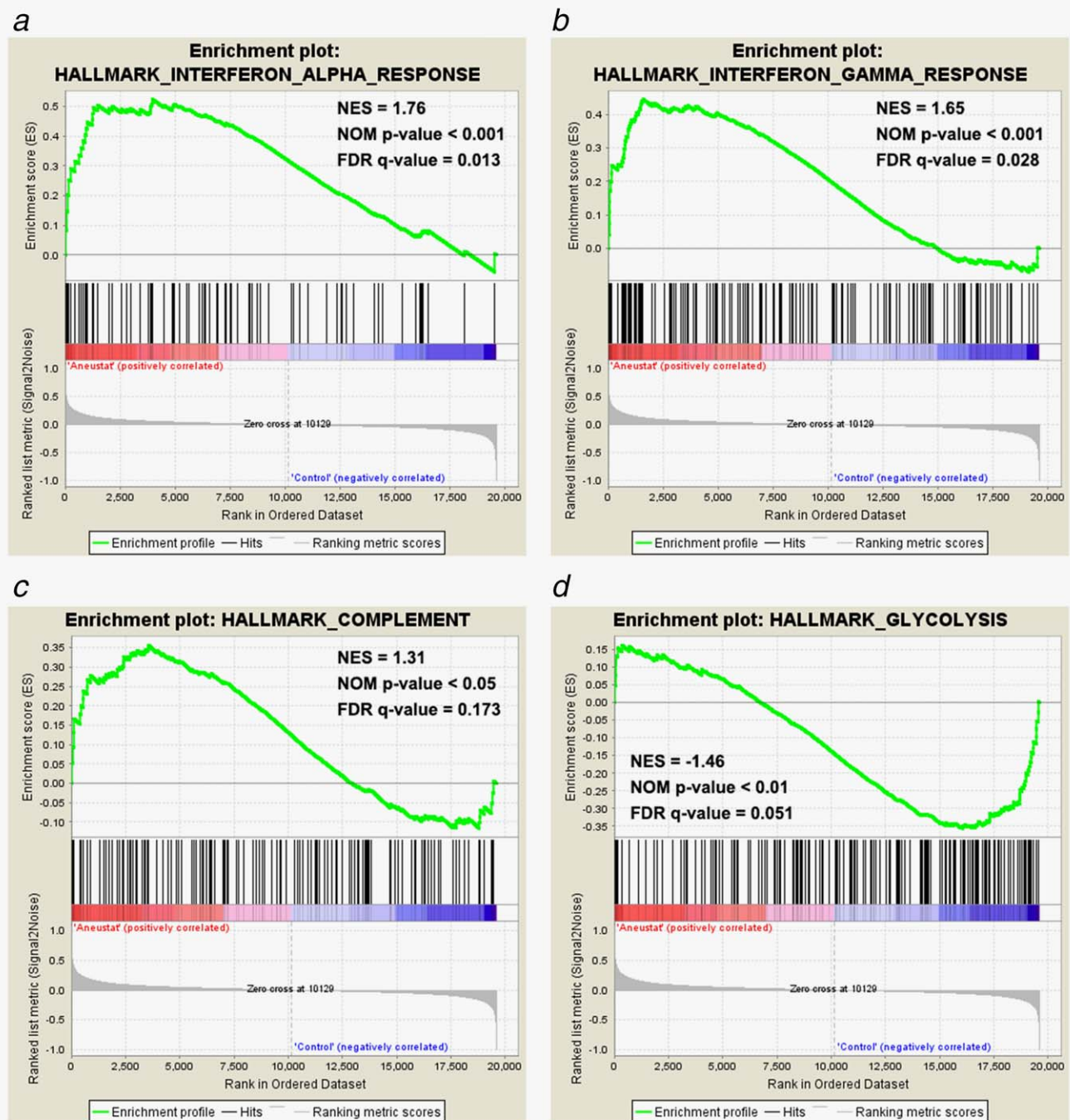
Cancer Therapy and Prevention

Figure 1. Enrichment of genes in Aneustat-treated LTL-313H xenografts relative to control. Gene enrichment in Aneustat-treated xenografts relative to controls was analyzed using GSEA hallmark gene-set signatures: (*a*) interferon-α response, (*b*) interferon-γ response, (*c*) complement and (*d*) glycolysis. [Color figure can be viewed at wileyonlinelibrary.com]

signatures. As shown in Figure 1, genes from the Aneustat-treated group were positively enriched in Interferon-α response, Interferon-γ response and Complement, but negatively enriched in Glycolysis. The data indicate that treatment with Aneustat positively correlates with immune response and negatively with cancer energy metabolism.

Inhibition by Aneustat of LNCaP cell proliferation and metabolism

LNCaP cells were incubated with vehicle control or Aneustat (200 μg/ml), an effective dosage as determined in a previous study;[24] live cell numbers were counted at 24 hr and 48 hr. Aneustat markedly inhibited the proliferation of LNCaP cells
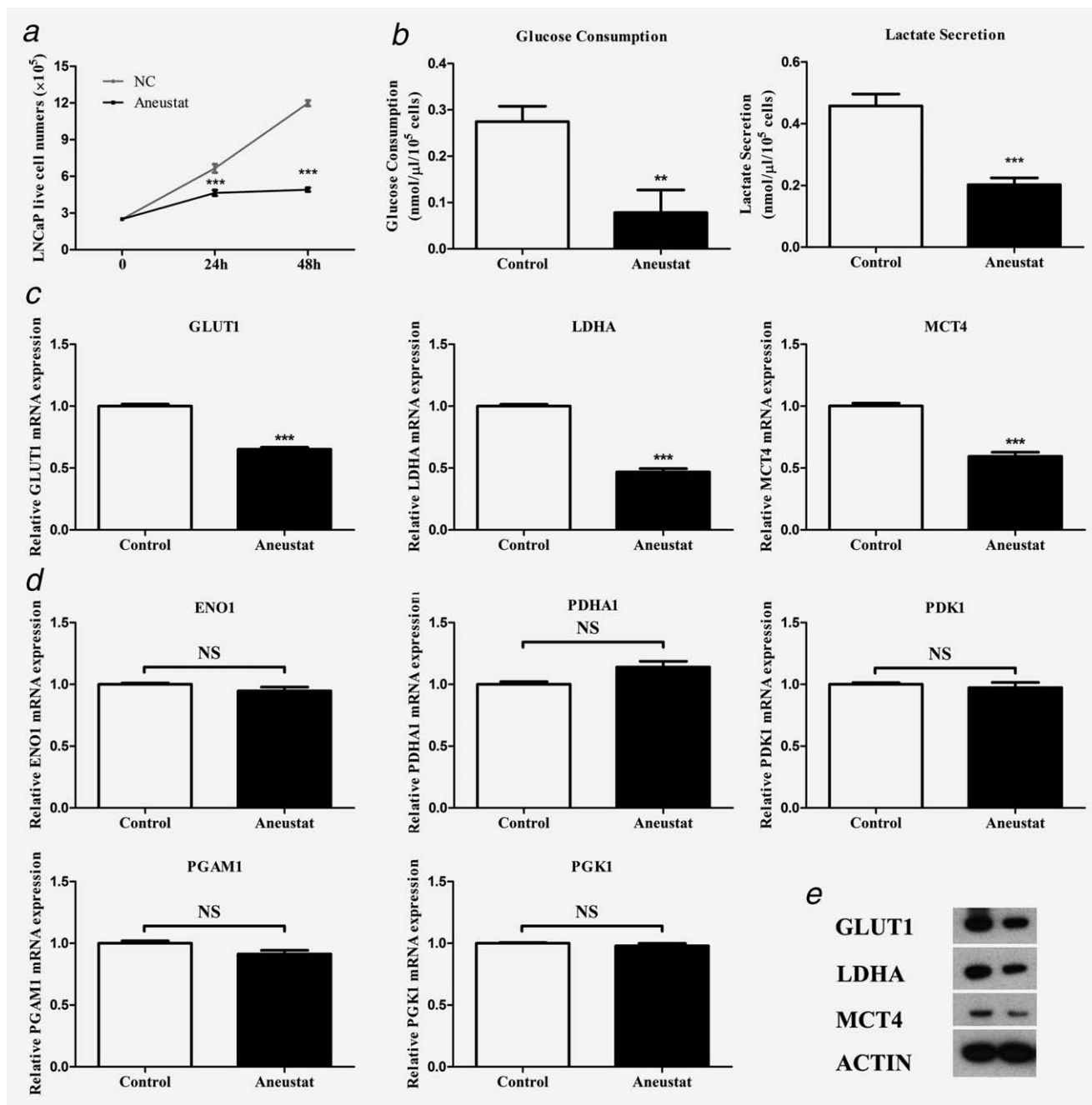
Figure 2. Effect of Aneustat on LNCaP cells. LNCaP prostate cancer cells were treated with Aneustat. Effect of Aneustat (200 μg/ml) on (*a*) cell numbers at 24 hr and 48 hr; (*b*) glucose consumption and lactate secretion at 48 hr; (*c* and *d*) mRNA expression of genes of the aerobic glycolysis pathway; (*e*) protein expression of GLUT1, LDHA and MCT4. The experiments were carried out independently (3×). **$p < 0.01$; ***$p < 0.001$; NS: not significant.

showing inhibitions of 30% and 59% at 24 hr and 48 hr, respectively (Fig. 2*a*). An 82% decrease in glucose consumption was observed, while lactate secretion was reduced by 56% (Fig. 2*b*). Furthermore, the mRNA and protein expressions of key genes in the aerobic glycolysis pathway, i.e. *GLUT1* (glucose transporter), *LDHA* (enzyme to convert pyruvate to lactate) and *MCT4* (lactate transporter) were markedly downregulated by Aneustat (Figs. 2*c* and 2*e*). Other genes in the aerobic glycolysis pathway (*ENO1, PDHA1,*

PDK1, PGAM1 and *PGK1*) were not affected by Aneustat (Fig. 2*d*). In contrast, the treatment with Aneustat led to upregulation of genes of the glutaminolysis pathway (Supporting Information Fig. S1).

Aneustat-induced differentiation of RAW264.7 macrophages to the M1 phenotype

Mouse RAW264.7 macrophages have been shown to exhibit a differentiation ability toward two phenotypes, M1 or M2: (i) their
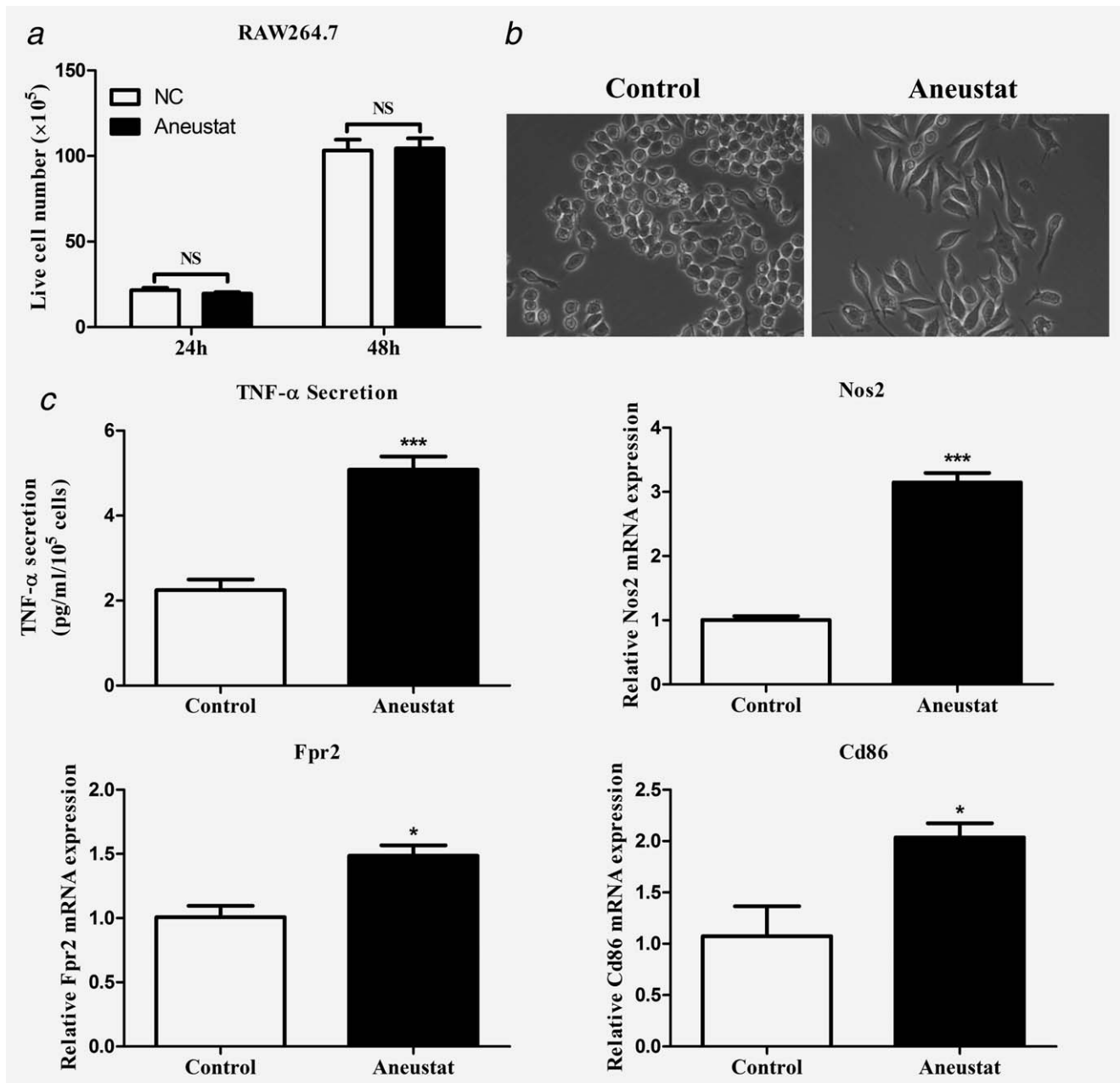
Cancer Therapy and Prevention

Figure 3. Effects of Aneustat on RAW264.7 macrophages. Mouse RAW264.7 macrophages were treated with Aneustat (200 µg/ml). Effect of Aneustat on (*a*) cell numbers at 24 hr and 48 hr; (*b*) cell morphology; (*c*) TNF-α secretion at 48 hr and the mRNA expressions of Nos2, Fpr2 and Cd86 at 24 hr. The experiments were carried out independently (3×). *$p < 0.05$; ***$p < 0.001$; NS: not significant.

treatment with antigens/cytokines, such as lipopolysaccharide (LPS), can induce the M1 phenotype associated with increased secretion of TNF-α (anticancer activity)[25] and (ii) treatment with IL-4 can lead to the M2 phenotype associated with increased secretion of TGF-β (pro-cancer activity).[26] In our study, treatment with Aneustat did not affect the proliferation of the RAW264.7 cells (Fig. 3*a*). However, Aneustat markedly changed the morphology of the cells from round to dendritic-like (Fig. 3*b*) and increased the secretion by the cells of TNF-α, a marker of the M1 phenotype (Fig. 3*c*). In addition, the mRNA expressions of M1 phenotype markers, such as Nos2,[27,28] Fpr2[29] and Cd86[30] were

significantly upregulated after Aneustat treatment of RAW264.7 cells (Fig. 3*c*). Together, these changes indicate that Aneustat induced differentiation of the RAW264.7 macrophages to the M1 anticancer phenotype.

Effect of Aneustat on the numbers of intratumoral mouse host immune cells in LNCaP cell xenografts

In our study, we showed that a 3-week treatment with Aneustat (1,652 mg/kg) of male athymic nude mice bearing subcutaneous LNCaP tumors markedly inhibited the growth of the tumors; there was no major host toxicity, as assessed by
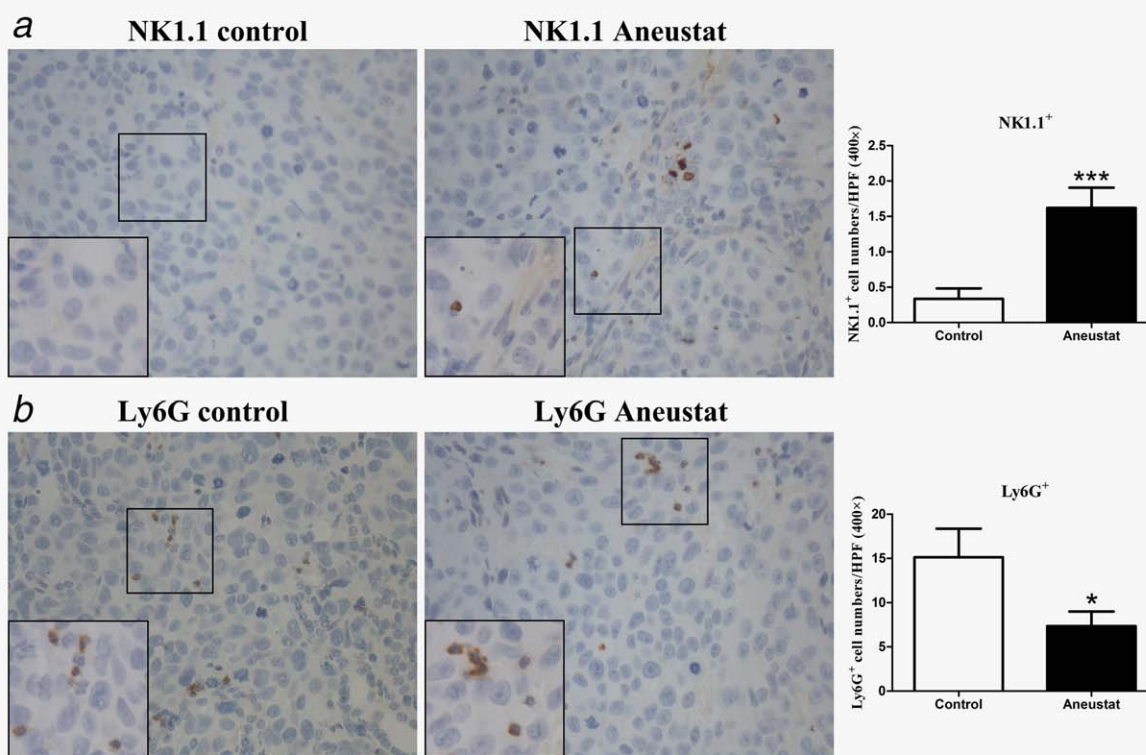
Figure 4. Effect of Aneustat on the relative levels of mouse NK1.1$^+$ cells and Ly6G$^+$ cells in LNCaP xenografts. Athymic nude mice bearing LNCaP xenografts were treated for 3 weeks with Aneustat (1,652 mg/kg) or vehicle control. The numbers of NK1.1$^+$ NK cells (*a*) and Ly6G$^+$ MDSCs (*b*) in the xenografts were counted using a 400× magnification. *$p < 0.05$; ***$p < 0.001$. [Color figure can be viewed at wileyonlinelibrary.com]

animal body weights and behavior.[18] Using preserved tissue sections of this experiment, the effect of Aneustat on the relative levels of mouse host NK cells and myeloid-derived suppressor cells (MDSCs) were determined by IHC, using NK1.1[31] and Ly6G[32] markers, respectively. As shown in Figure 4, the relative numbers of intratumoral NK1.1$^+$ NK cells, the major functional cytotoxic immune cell subtype in nude mice,[33] were markedly higher in the Aneustat-treated than in the control tissues; in contrast, the numbers of MDSCs, the immunosuppressive cells,[34] were significantly lower in the Aneustat-treated than in the control tissues. The data show that treatment with Aneustat can increase the intratumoral levels of host anticancer immune cells and reduce the intratumoral levels of host immunosuppressive cells.

Effect of Aneustat on the numbers of intratumoral patient immune cells in first-generation patient-derived prostate cancer tissue xenografts

To investigate whether treatment with Aneustat has an effect on the relative levels of intratumoral patient immune cells, a first-generation patient-derived xenograft model of metastatic prostate cancer tissue was used (subsequent generations of xenografts would have been deficient in human immune cells). To this end, the xenograft-bearing mice were treated, 10 days after grafting, for 3 weeks with vehicle control or

Aneustat (1,652 mg/kg), an effective, non-toxic dosage determined in our study.[18] No major host toxicity was observed. Quantification of patient immune cells in the xenograft tissues that positively stained for various human immune cell markers was used to assess the effect of Aneustat. As shown in Figure 5a, Aneustat did not have a significant effect on the relative numbers of intratumoral patient CD8$^+$ cytotoxic T cells. In contrast, as shown in Figure 5b, Aneustat very markedly reduced the numbers of FOXP3$^+$ Treg cells (by >90%), thereby markedly increasing the ratio of intratumoral patient anticancer T cells to Treg cells in the Aneustat-treated tissues. NK cells and MDSCs were identified by staining with NCR1 and CD33, respectively.[35–37] As shown in Figure 6, the Aneustat-treated tissues showed higher NCR1$^+$ NK cell numbers compared to controls, whereas the MDSCs in the Aneustat-treated tissues were lower in number than in the controls. Taken together, the data show that treatment of the first-generation metastatic prostate cancer xenografts with Aneustat was associated with an increase in the numbers of patient anticancer immune cells and a decrease in the numbers of patient immunosuppressive cells.

Discussion

Our study has demonstrated that Aneustat can markedly inhibit LNCaP prostate cancer growth *in vitro*, consistent
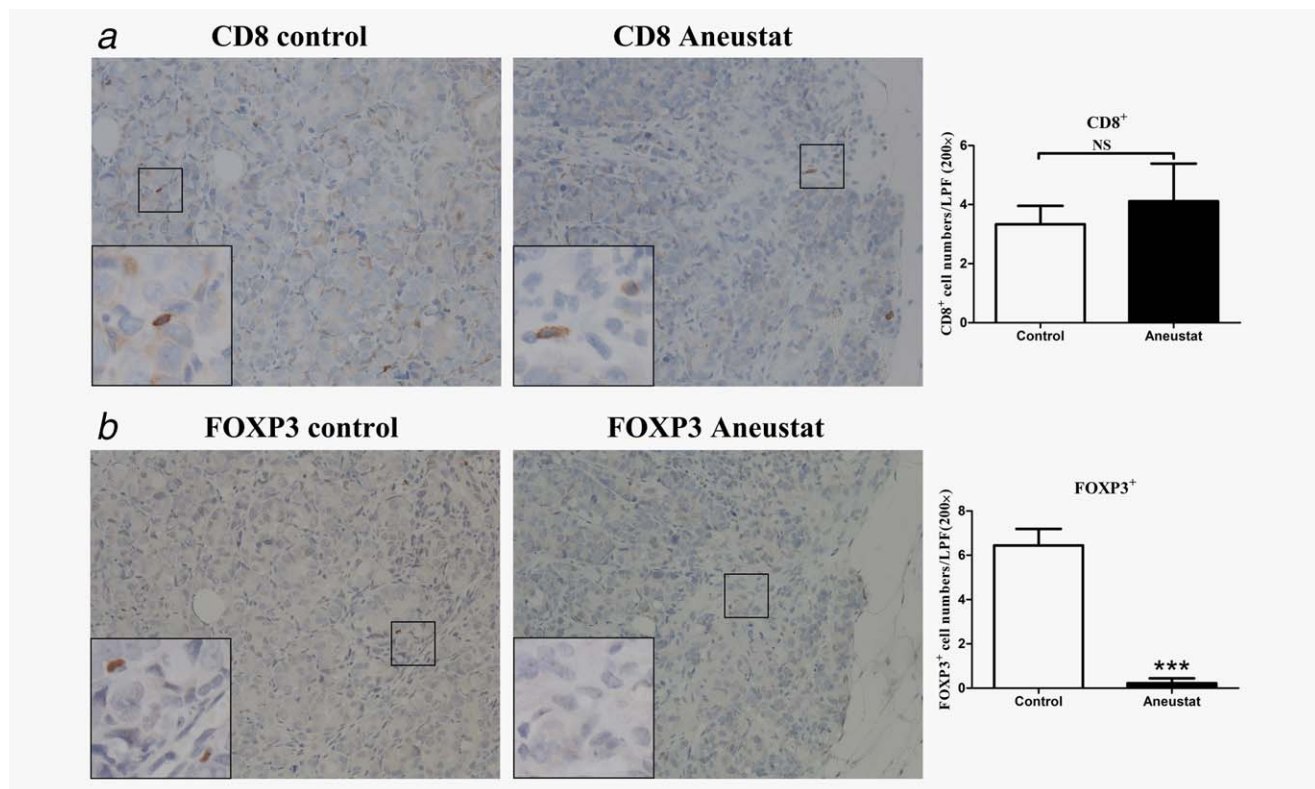
Cancer Therapy and Prevention

Figure 5. Effect of Aneustat on the relative levels of human CD8+ cells and FOXP3+ cells in first-generation patient-derived prostate cancer tissue xenografts. NSG mice bearing first-generation prostate cancer tissue xenografts were treated for 3 weeks with Aneustat (1,652 mg/kg) or vehicle control. (a) The number of CD8+ T cells and (b) FOXP3+ Treg cells in the xenografts were determined using a 200× magnification. ***$p < 0.001$; NS: not significant. [Color figure can be viewed at wileyonlinelibrary.com]

with previously reported findings.[17,18] The arrest of LNCaP cell proliferation by Aneustat is likely a result of its inhibition of aerobic glycolysis (Figs. 2a–2c and 2e). Thus, as shown in Figure 2, *in vitro* incubation of LNCaP cells with Aneustat led to substantial decreases in glucose consumption (∼82%), lactic acid secretion (∼56%) and downregulation of expression of major glycolysis-related genes, i.e. *GLUT1* (encoding the glucose transporter), *LDHA* (encoding lactate dehydrogenase A) and *MCT4* (encoding a major plasma membrane transporter of cancer-generated lactic acid[8]). The finding that Aneustat led to upregulation of genes of the glutaminolysis pathway (Supporting Information Fig. S1), suggests that this pathway was used by the LNCaP cells as an alternative route to generate more lactate. However, as the amount of glutaminolysis-generated lactate in general is much smaller than the amount of lactate generated via aerobic glycolysis,[38–40] it would not greatly affect the inhibition by Aneustat of lactic acid secretion (Fig. 2b). The finding that Aneustat inhibited the aerobic glycolysis of LNCaP prostate cancer cells confirms the gene set enrichment by GSEA results that treatment with Aneustat is negatively correlated with cancer cell glycolytic activity (Fig. 1d). As cancer growth greatly relies on aerobic glycolysis,[41,42] the inhibition of aerobic glycolysis by Aneustat could be a major mechanism by which it

inhibits the proliferation of LNCaP prostate cancer cells *in vitro* and *in vivo*.

Although Aneustat markedly inhibited the growth of LNCaP cell xenografts, it did not significantly inhibit the growth of patient-derived LTL-313H prostate cancer xenografts as we previously reported.[18] This discrepancy may tentatively be explained by basic differences between the two mouse models. The LNCaP xenograft model is based on nude, immuno-compromised mice that still contain functional cytotoxic NK cells.[33] In contrast, the LTL-313H PDX model is based on immunodeficient mice totally lacking functional immune cells. In our study, treatment with Aneustat was found to favor the host anticancer immune response. Consequently, the growth inhibition by Aneustat of the LNCaP xenografts may be based – to some extent – on Aneustat-induced stimulation of cytotoxic NK cells. Other differences that play a role may include differences in responses to Aneustat between LTL-313H and LNCaP prostate cancer cells and greater cancer heterogeneity in the LTL-313H xenografts.

Historically, Chinese herbal preparations have been shown to possess medicinal benefits, including stimulation of the immune system.[43] In our study, it was found that Aneustat has immunomodulatory activity. Thus treatment
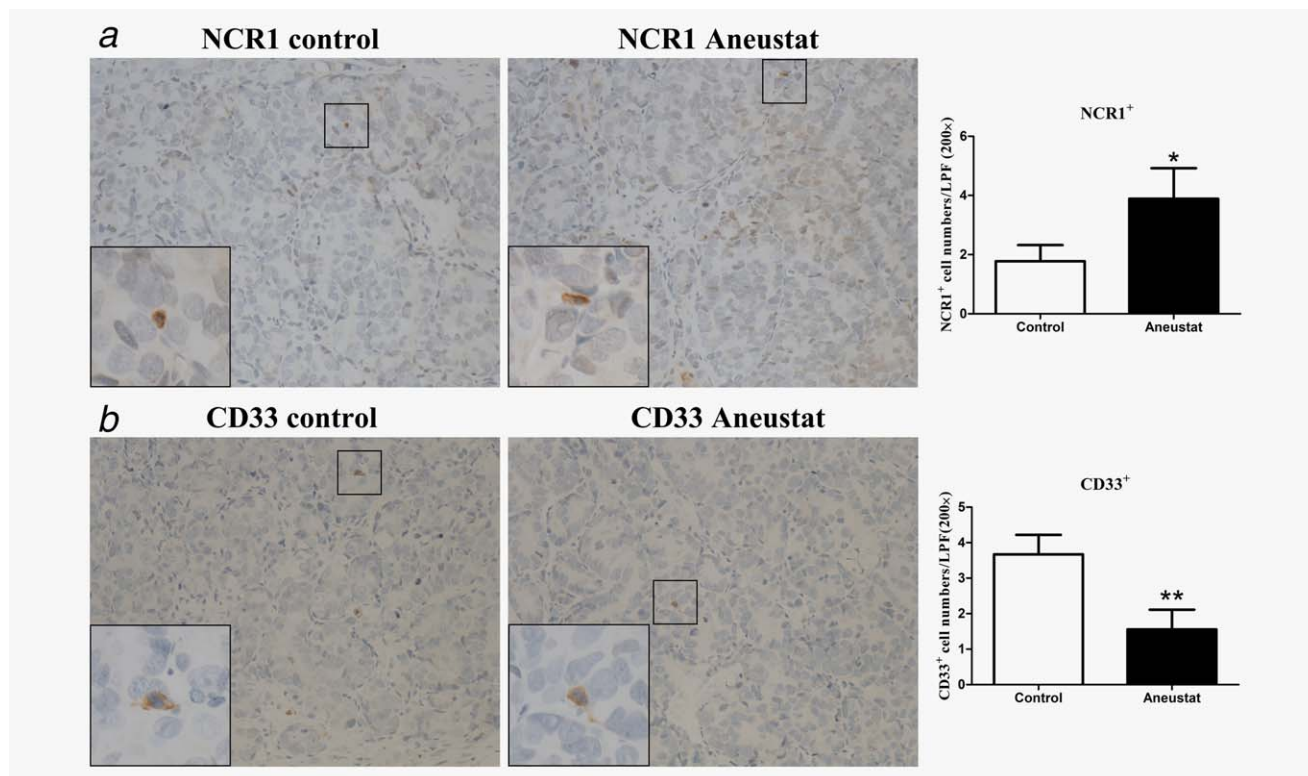
Figure 6. Effect of Aneustat on the relative levels of human NCR1^{+} cells and CD33^{+} cells in first-generation patient-derived prostate cancer tissue xenografts. NSG mice bearing first-generation prostate cancer tissue xenografts were treated for 3 weeks with Aneustat (1,652 mg/kg) or vehicle control. (*a*) The numbers of NCR1^{+} NK cells and (*b*) the number of CD33^{+} MDSCs in the xenografts were counted using a 200× magnification. *$p < 0.05$; **$p < 0.01$. [Color figure can be viewed at wileyonlinelibrary.com]

with Aneustat led to differentiation of RAW264.7 macrophages to the M1 anticancer phenotype (Fig. 3). Importantly, treatment with Aneustat of metastatic prostate cancer tissue xenografts and LNCaP xenografts led in both cases to marked changes in the levels of intratumoral host (patient/mouse) immune cells favoring the host anticancer immune response, i.e. a higher ratio of intratumoral cytotoxic T cells/Treg cells, higher numbers of intratumoral NK cells and lower numbers of intratumoral MDSCs (Figs. 4–6). Similar changes in the levels of host immune cells have been reported for mouse melanoma allografts in immunocompetent mice when their lactic acid secretion was reduced (via specific depletion of glycolysis-related LDHA the enzyme involved in the conversion of pyruvate to lactate).[10] In view of this, it appears likely that the immunomodulatory activity of Aneustat is based on reduction of cancer-generated lactic acid secretion as obtained via aerobic glycolysis inhibition (Fig. 2). As such, our study shows, for the first time, that Aneustat has immunomodulatory properties based on (i) ability to induce macrophage differentiation, and (ii) inhibition of aerobic glycolysis leading to reduced secretion of cancer-generated lactic acid. The data are consistent with the GSEA results of the microarray data of LTL-313H xenografts indicating that Aneustat affected the immune response (Figs. 1*a*–1*c*).

Since treatment with Aneustat appears to favor the host anticancer immune response, as indicated by our study, it may lead to reduction of cancer-induced immunosuppression in immunocompetent hosts. This suggestion is supported by the finding in the Aneustat Phase-I clinical trial that treatment with Aneustat led to a reduction in the levels of immune suppression markers in patients.[16] Further studies are needed to establish the mechanisms of action underlying the immunomodulatory activity of Aneustat. Restoration of the host anticancer immune response by Aneustat should be beneficial for potential clinical therapy of advanced prostate cancers using docetaxel combined with Aneustat, as previously reported.[18]

Patient-derived xenograft (PDX) cancer models are becoming widely used in cancer research, in particular subrenal capsule xenografts which show high fidelity to the original patient tumors with regard to histopathology, tumor heterogeneity, tissue architecture, gene expression profiles and tumor aggressiveness.[44] The main limitation of PDX models is the absence of a functional immune system, making them unsuitable for comprehensive immunological studies.[45] However, as shown by our study, first-generation PDX models contain a variety of tumor-infiltrated patient immune cells (Figs. 5 and 6), as distinct from later generation models that do not have this feature,

Cancer Therapy and Prevention

since patient immune cells vanish on serial propagation of the xenografts. As such, first-generation PDX models may provide use for limited immunological studies such as investigations of the effect of candidate drugs on the levels of the patient immune cells. They may find application in screening drugs/compounds for immunomodulatory properties.

In conclusion, our study has shown that Aneustat has immunomodulatory activity, as indicated, in particular, by its induction of a shift in the levels of intratumoral host immune cells which favor the host anticancer immune response. This immunomodulatory activity appears to be based on Aneustat-induced inhibition of aerobic glycolysis leading to a reduction in the secretion of cancer-generated lactic acid and hence reduced acidification of the tumor microenvironment.

Furthermore, first-generation patient-derived cancer tissue xenograft models may be used for screening immunomodulatory activity of compounds.

Authors' Contributions

- Conception, design and study supervision: Yuzhuo Wang
- Acquisition of data: Sifeng Qu, Hui Xue, Xin Dong, Rebecca Wu, Noushin Nabavi
- Analysis and interpretation of data: Sifeng Qu, Peter W. Gout, Xin Dong, Dong Lin, Hui Xue, Yuzhuo Wang
- Drafting/final approval of the manuscript: Sifeng Qu, Peter W. Gout, Colin C. Collins, Martin E. Gleave, Yuzhuo Wang

References

1. Zamarron BF, Chen W. Dual roles of immune cells and their factors in cancer development and progression. *Int J Biol Sci* 2011;7:651–8.
2. Kim R, Emi M, Tanabe K. Cancer immunoediting from immune surveillance to immune escape. *Immunology* 2007;121:1–14.
3. Dunn GP, Old LJ, Schreiber RD. The three Es of cancer immunoediting. *Annu Rev Immunol* 2004; 22:329–60.
4. Ostrand-Rosenberg S. Immune surveillance: a balance between protumor and antitumor immunity. *Curr Opin Genet Dev* 2008;18:11–8.
5. Whiteside TL. Inhibiting the inhibitors: evaluating agents targeting cancer immunosuppression. *Expert Opin Biol Ther* 2010;10:1019–35.
6. Stewart TJ, Smyth MJ. Improving cancer immunotherapy by targeting tumor-induced immune suppression. *Cancer Metastasis Rev* 2011;30:125–40.
7. Choi SY, Collins CC, Gout PW, et al. Cancer-generated lactic acid: a regulatory, immunosuppressive metabolite? *J Pathol* 2013;230:350–5.
8. Choi SY, Xue H, Wu R, et al. The MCT4 gene: a novel, potential target for therapy of advanced prostate cancer. *Clin Cancer Res* 2016;22:2721–33.
9. Husain Z, Huang Y, Seth P, et al. Tumor-derived lactate modifies antitumor immune response: effect on myeloid-derived suppressor cells and NK cells. *J Immunol* 2013;191:1486–95.
10. Brand A, Singer K, Koehl GE, et al. LDHA-associated lactic acid production blunts tumor immunosurveillance by T and NK cells. *Cell Metab* 2016;24:657–71.
11. Liu C, Workman CJ, Vignali DA. Targeting regulatory T cells in tumors. *FEBS J* 2016;283:2731–48.
12. Pasero C, Gravis G, Granjeaud S, et al. Highly effective NK cells are associated with good prognosis in patients with metastatic prostate cancer. *Oncotarget* 2015;6:14360–73.
13. Sato E, Olson SH, Ahn J, et al. Intraepithelial CD8+ tumor-infiltrating lymphocytes and a high CD8+/regulatory T cell ratio are associated with favorable prognosis in ovarian cancer. *Proc Natl Acad Sci U S A* 2005;102:18538–43.
14. Gao Q, Qiu SJ, Fan J, et al. Intratumoral balance of regulatory and cytotoxic T cells is associated with prognosis of hepatocellular carcinoma after resection. *JCO* 2007;25:2586–93.

15. Vasievich EA, Huang L. The suppressive tumor microenvironment: a challenge in cancer immunotherapy. *Mol Pharm* 2011;8:635–41.
16. Renouf D, Kollmannsberger C, Chi K, et al. Abstract C41: a Phase 1 study of OMN54 in patients with advanced malignancies. *Mol Cancer Ther* 2015;14:C41–C.
17. Mikovits JA, Gerwick L, Oroudjev E, et al. Preclinical development of Aneustat (OMN54): a multifunctional multi-targeted natural product derivative with anti-tumor, anti-inflammatory and immuno-modulatory activity. *Mol Cancer Ther* 2007;6:3548s–s.
18. Qu S, Wang K, Xue H, et al. Enhanced anticancer activity of a combination of docetaxel and Aneustat (OMN54) in a patient-derived, advanced prostate cancer tissue xenograft model. *Mol Oncol* 2014;8:311–22.
19. Subramanian A, Tamayo P, Mootha VK, et al. Gene set enrichment analysis: a knowledge-based approach for interpreting genome-wide expression profiles. *Proc Natl Acad Sci U S A* 2005;102: 15545–50.
20. Mootha VK, Lindgren CM, Eriksson KF, et al. PGC-1alpha-responsive genes involved in oxidative phosphorylation are coordinately downregulated in human diabetes. *Nat Genet* 2003;34:267–73.
21. Wang Y, Xue H, Cutz JC, et al. An orthotopic metastatic prostate cancer model in SCID mice via grafting of a transplantable human prostate tumor line. *Lab Invest* 2005;85:1392–404.
22. Salgado R, Denkert C, Demaria S, et al. The evaluation of tumor-infiltrating lymphocytes (TILs) in breast cancer: recommendations by an International TILs Working Group 2014. *Ann Oncol* 2015;26:259–71.
23. Garg K, Soslow RA. Lynch syndrome (hereditary non-polyposis colorectal cancer) and endometrial carcinoma. *J Clin Pathol* 2009;62:679–84.
24. Qu S, Ci X, Xue H, et al. Treatment with docetaxel in combination with Aneustat leads to potent inhibition of metastasis in a patient-derived xenograft model of advanced prostate cancer. *Br J Cancer* 2018.
25. Huang BP, Lin CH, Chen YC, et al. Anti-inflammatory effects of Perilla frutescens leaf extract on

lipopolysaccharide-stimulated RAW264.7 cells. *Mol Med Rep* 2014;10:1077–83.
26. Mandal P, Pratt BT, Barnes M, et al. Molecular mechanism for adiponectin-dependent M2 macrophage polarization: link between the metabolic and innate immune activity of full-length adiponectin. *J Biol Chem* 2011;286: 13460–9.
27. Mantovani A, Sica A, Sozzani S, et al. The chemokine system in diverse forms of macrophage activation and polarization. *Trends Immunol* 2004;25:677–86.
28. Watschinger K, Keller MA, McNeill E, et al. Tetrahydrobiopterin and alkylglycerol monooxygenase substantially alter the murine macrophage lipidome. *Proc Natl Acad Sci U S A* 2015;112: 2431–6.
29. Liu Y, Chen K, Wang C, et al. Cell surface receptor FPR2 promotes antitumor host defense by limiting M2 polarization of macrophages. *Cancer Res* 2013;73:550–60.
30. Gensel JC, Kopper TJ, Zhang B, et al. Predictive screening of M1 and M2 macrophages reveals the immunomodulatory effectiveness of post spinal cord injury azithromycin treatment. *Sci Rep* 2017; 7:40144.
31. Orr MT, Beilke JN, Proekt I, et al. Natural killer cells in NOD.NK1.1 mice acquire cytolytic function during viral infection and provide protection against cytomegalovirus. *Proc Natl Acad Sci U S A* 2010;107:15844–9.
32. Bronte V, Brandau S, Chen SH, et al. Recommendations for myeloid-derived suppressor cell nomenclature and characterization standards. *Nat Commun* 2016;7:12150.
33. Shultz LD, Ishikawa F, Greiner DL. Humanized mice in translational biomedical research. *Nat Rev Immunol* 2007;7:118–30.
34. Gabrilovich DI, Ostrand-Rosenberg S, Bronte V. Coordinated regulation of myeloid cells by tumours. *Nat Rev Immunol* 2012;12: 253–68.
35. Hadad U, Thauland TJ, Martinez OM, et al. NKp46 clusters at the immune synapse and regulates NK cell polarization. *Front Immunol* 2015;6: 495.
36. Sivori S, Pende D, Bottino C, et al. NKp46 is the major triggering receptor involved in the natural cytotoxicity of fresh or cultured human NK cells.

Correlation between surface density of NKp46 and natural cytotoxicity against autologous, allogeneic or xenogeneic target cells. *Eur J Immunol* 1999;29:1656–66.

37. Gielen PR, Schulte BM, Kers-Rebel ED, et al. Increase in both CD14-positive and CD15-positive myeloid-derived suppressor cell subpopulations in the blood of patients with glioma but predominance of CD15-positive myeloid-derived suppressor cells in glioma tissue. *J Neuropathol Exp Neurol* 2015;74:390–400.

38. Israelsen WJ, Dayton TL, Davidson SM, et al. PKM2 isoform-specific deletion reveals a differential requirement for pyruvate kinase in tumor cells. *Cell* 2013;155:397–409.

39. Scott DA, Richardson AD, Filipp FV, et al. Comparative metabolic flux profiling of melanoma cell lines: beyond the Warburg effect. *J Biol Chem* 2011;286:42626–34.

40. Montal ED, Dewi R, Bhalla K, et al. PEPCK coordinates the regulation of central carbon metabolism to promote cancer cell growth. *Mol Cell* 2015;60:571–83.

41. Vander Heiden MG, Cantley LC, Thompson CB. Understanding the Warburg effect: the metabolic requirements of cell proliferation. *Science* 2009; 324:1029–33.

42. Ward PS, Thompson CB. Metabolic reprogramming: a cancer hallmark even Warburg did not anticipate. *Cancer Cell* 2012;21:297–308.

43. Ma HD, Deng YR, Tian Z, et al. Traditional Chinese medicine and immune regulation. *Clin Rev Allergy Immunol* 2013;44:229–41.

44. Lin D, Wyatt AW, Xue H, et al. High fidelity patient-derived xenografts for accelerating prostate cancer discovery and drug development. *Cancer Res* 2014;74:1272–83.

45. Aparicio S, Hidalgo M, Kung AL. Examining the utility of patient-derived xenograft mouse models. *Nat Rev Cancer* 2015;15:311–6.

Cancer Therapy and Prevention